Meander-Line and Hybrid Meander-Line Transformers

EDWARD G. CRISTAL

Abstract—**The application of meander lines to impedance transformers is described. Meander-line transformers have less bandwidth than stepped-impedance transformers for a given passband VSWR, but can have greatly superior shape factors in stripline and microwave-integrated-circuit (MIC) realizations. Hybrid meander-line transformers allow circuit designers greatly increased flexibility in choosing transformer shape factors, while allowing (basically) the same electrical performance as with either stepped-impedance or meander-line transformers. Experimental confirmations of a trial three-turn meander-line transformer and a fourth-order hybrid meander-line transformer are presented. A comprehensive design table of nearly equal-ripple meander-line transformers of from two to six turns, incorporating a wide range of bandwidths and impedance transformations has been deposited with the ASIS National Auxiliary Publications Service.**

I. Introduction

TRANSFORMERS are very often required in microwave components and systems. Coupled transmission-line geometries, such as interdigital and/or combine, are often used for purposes of obtaining impedance transformations [1]. However, in many applications these structures are quite unsatisfactory for the following reasons. 1) The required coupling between lines may not be practically realized. 2) One or more of the coupled lines may require grounding, which is difficult in stripline and microwave-integrated-circuit (MIC) realizations. 3) The equivalent circuits for these and other coupled-line geometries contain, in addition to ideal transformers, shunt or series reactances that limit the bandwidth over which the transformer may be used.

The stepped-impedance transformer [2]–[4], consisting of a cascade of unit elements (UE) [5], is also commonly used. The stepped-impedance transformer can transform widely differing impedances (resistances, to be strictly correct) over narrow to very wide bandwidths and it can be constructed readily in airline, stripline, and MIC. However, each section of a stepped-impedance transformer is a quarter-wavelength long at band center.[1] Consequently, the length of a multisection transformer can be quite large. For example, a three-section stripline transformer constructed on Rexolite 1422 ($\epsilon_r = 2.54$) centered at 1000 MHz would be 5.56 in long. If, as is sometimes the case, transformers are required at both the input and output of a device, the overall length of the stepped-impedance transformers and device could be excessive. An idealized solution to this problem would be to fold the stepped-impedance transformer accordion fashion, as illustrated in Fig. 1. In order to preserve the electrical characteristics of the circuit, shielding between the folded lines would be needed. Conceptually, this technique is satisfactory, but in practice the required shielding would be impractical. On the other hand, if the shields were removed, there would be sufficient coupling between lines to seriously degrade the transformer performance.

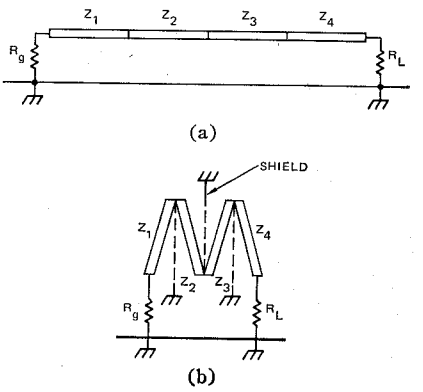

Fig. 1. Stepped-impedance transformers. (a) Unfolded. (b) Folded.

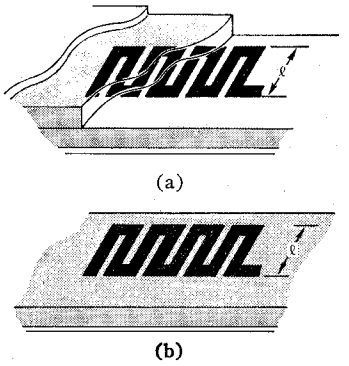

Fig. 2. Conventional meander-line geometries. (a) Stripline. (b) Microwave integrated circuit (MIC).

Fig. 2 depicts conventional meander-line geometries in stripline and MIC. We note that these structures may be considered as folded coupled-line stepped-impedance lines. Thus, from this perspective, the meander line might be considered as comprising a class of generalized coupled-line transformers within which the stepped-impedance transformer is merely a special case for which coupling between turns is negligible. From this point of view, an extension of meander-line transformers to hybrid meander-line transformers is quite natural. *A hybrid meander-line transformer is one in which coupling between some adjacent turns is negligible, whereas for other adjacent turns it is significant.* Several examples of hybrid meander-line transformers are given in Fig. 3. Theoretically, the number of hybrid configurations is $2(N-1)$, where N is the order of the transformer. Hybrid geometries allow the circuit designer much greater flexibility in the physical layout of the trans-

Manuscript received April 11, 1972; revised September 13, 1972. This work was supported by the U. S. Army Electronics Command Laboartory under Contract DAAB07-70-C-0044. This paper was presented at the 1972 G-MTT International Symposium, Washington, D. C.

The author was with Stanford Research Institute, Menlo Park, Calif. He is now with McMaster University and the Communications Research Laboratory, Hamilton, Ont., Canada.

[1] Excepting the short-step transformer [6].

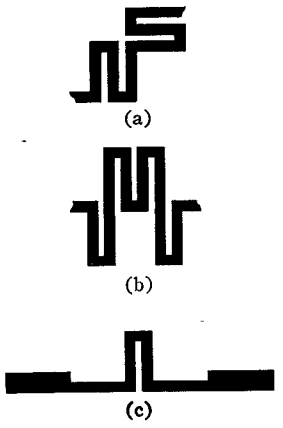

Fig. 3. Hybrid meander-line geometries. (a) Example 1. (b) Example 2. (c) Example 3.

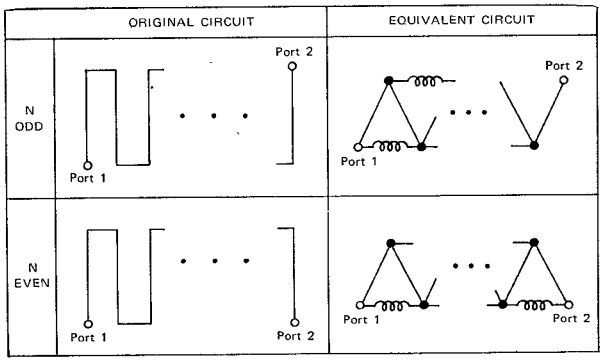

Fig. 4. Two-port equivalent circuits for meander lines having negligible coupling between nonadjacent turns.

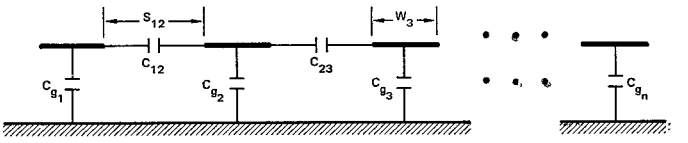

Fig. 5. Schematic cross-sectional representation for meander-line transformers.

TABLE I

MEANDER-LINE TRANSFORMER DESIGNS

PROGRAM BY E.G. CRISTAL OCTOBER 1971

3 SECTION MEANDER-LINE TRANSFORMER TABLE
CAPACITANCES NORMALIZED TO 376.7/SQRT(EPSR)
COUPLING = 10 TO 16 DB
BANDWIDTH = 3.00/1.

RL/RG	CG1/E	CG2/E	CG3/E	CM12/E	CM23/E	VSWR
1.0	.8638	.6407	.7350	.1334	.3056	1.028
1.1	.8485	.6205	.6973	.1403	.2857	1.025
1.2	.8203	.5877	.6516	.1406	.2617	1.051
1.3	.8089	.5732	.6215	.1358	.2361	1.078
1.4	.7895	.5559	.5962	.1387	.2153	1.096
1.5	.7759	.5415	.5701	.1352	.1999	1.114
1.6	.7661	.5326	.5484	.1250	.1783	1.129
1.7	.7573	.5265	.5324	.1235	.1605	1.145
1.8	.7504	.5208	.5171	.1176	.1434	1.157
1.9	.7406	.5144	.5035	.1150	.1277	1.167
2.0	.7275	.5185	.5036	.1221	.1004	1.173
2.2	.7230	.5061	.4659	.1105	.8817E-01	1.220
2.4	.7109	.4828	.4387	.1020	.8543E-01	1.226
2.6	.6991	.4701	.4175	.9746E-01	.7481E-01	1.240
2.8	.6917	.4566	.3957	.9516E-01	.7181E-01	1.268
3.0	.6766	.4362	.3730	.9228E-01	.7028E-01	1.288
3.5	.6519	.4075	.3342	.8588E-01	.6191E-01	1.326
4.0	.6302	.3757	.2941	.7795E-01	.6389E-01	1.391
4.5	.6142	.3608	.2765	.7626E-01	.5120E-01	1.414
5.0	.5979	.3413	.2542	.7155E-01	.4730E-01	1.457
6.0	.5708	.3125	.2217	.6851E-01	.4117E-01	1.550

PROGRAM BY E.G. CRISTAL OCTOBER 1971

4 SECTION MEANDER-LINE TRANSFORMER TABLE
CAPACITANCES NORMALIZED TO 376.7/SQRT(EPSR)
COUPLING = 10 TO 16 DB
BANDWIDTH = 3.00/1.

RL/RG	CG1/E	CG2/E	CG3/E	CG4/E	CM12/E	CM23/E	CM34/E	VSWR
1.0	.8551	.7455	.7433	.8526	.1591	.1368	.1621	1.000
1.1	.8269	.6817	.6690	.7761	.1755	.1659	.1638	1.014
1.2	.8122	.6666	.6516	.7287	.1772	.1440	.1430	1.027
1.3	.8151	.6589	.6209	.6789	.1589	.1344	.1360	1.039
1.4	.8114	.6421	.5926	.6391	.1503	.1329	.1204	1.050
1.5	.8062	.6294	.5696	.6026	.1443	.1257	.1194	1.060
1.6	.7979	.6147	.5483	.5704	.1423	.1202	.1139	1.068
1.7	.7941	.6043	.5297	.5424	.1363	.1151	.1079	1.075
1.8	.7864	.5908	.5128	.5178	.1351	.1116	.1021	1.082
1.9	.7832	.5821	.4973	.4948	.1303	.1070	.9729E-01	1.089
2.0	.7757	.5699	.4826	.4744	.1298	.1041	.9295E-01	1.095
2.2	.7662	.5516	.4562	.4382	.1247	.9820E-01	.8567E-01	1.107
2.4	.7566	.5351	.4334	.4076	.1213	.9283E-01	.7974E-01	1.118
2.6	.7484	.5203	.4134	.3814	.1176	.8843E-01	.7439E-01	1.129
2.8	.7406	.5068	.3955	.3587	.1144	.8477E-01	.6980E-01	1.139
3.0	.7337	.4946	.3794	.3386	.1109	.8138E-01	.6580E-01	1.148
3.5	.7171	.4678	.3469	.2987	.1057	.7480E-01	.5730E-01	1.168
4.0	.7022	.4465	.3208	.2672	.1022	.6816E-01	.5172E-01	1.189
4.5	.6900	.4274	.2985	.2421	.9739E-01	.6390E-01	.4710E-01	1.206
5.0	.6794	.4112	.2800	.2219	.9319E-01	.6037E-01	.4323E-01	1.223
6.0	.6600	.3841	.2514	.1913	.8787E-01	.5481E-01	.3697E-01	1.255
7.0	.6452	.3633	.2293	.1686	.8227E-01	.5040E-01	.3284E-01	1.283
8.0	.6300	.3451	.2114	.1510	.7877E-01	.4667E-01	.2944E-01	1.310
9.0	.6183	.3305	.1973	.1373	.7525E-01	.4372E-01	.2678E-01	1.334
10.0	.6077	.3179	.1857	.1262	.7278E-01	.4122E-01	.2463E-01	1.358
20.0	.5429	.2507	.1263	.7344E-01	.5883E-01	.2738E-01	.1443E-01	1.550

former than he would otherwise have with only meander-line and stepped-impedance transformers.

The meander line is not a new transmission-line geometry. Butcher [7] studied it from the point of view of its possible application in traveling-wave tubes. Bolljahn and Matthaei [8] computed its image impedance in the general all coupled-line case and Hewitt [9] utilized the structure in a microwave compression filter. The most recent and novel treatment of the meander line has been given by Sato [10]. An equivalent circuit for meander lines (presented by Sato) having coupling only between adjacent turns is given in Fig. 4. The coupling between turns is accounted for solely by "S-plane inductors" [5], [11] connecting unit elements. A stepped-impedance geometry is obtained by setting all inductive admittance values to zero. A hybrid geometry is obtained by setting some but not all inductive admittance values to zero. The equivalent circuit of Fig. 4 forms the basis for the compilation of meander-line transformer designs given later.

II. Meander-Line Transformer Design Tables

The meander-line transformer tables presented later in this section were compiled using numerical techniques by minimizing a *weighted* reflection-coefficient function raised to a high integer power (e.g., minimizing a least-pth objective). The weighting function was constructed to assure that the coupling between meander-line turns would be within prescribed practical limits selected by the user. The numerical

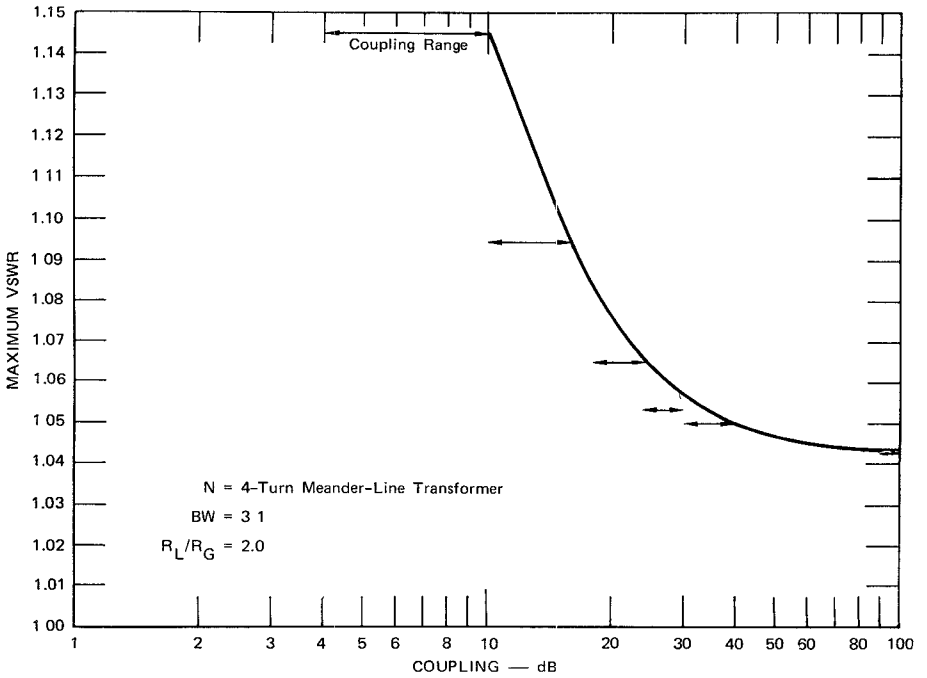

Fig. 6. Variation of peak VSWR for various coupling values between meander-line turns.

techniques are well known [12] and, consequently, specific details will not be given here.

A. Definition of Parameters Used in Design Tables

Fig. 5 depicts a cross-sectional representation of an arbitrary meander-line transformer in any TEM or quasi-TEM medium and depicts the unnormalized distributed capacitance parameters C_{g_i} and $C_{i,i+1}$. These are defined as follows:

C_{gi} capacitance to ground per unit length for the ith conductor

$C_{i,i+1}$ mutual capacitance per unit length between the ith and ith + 1 conductors. (1)

Coupling between nonadjacent lines is assumed negligible.

The dimensionless distributed-capacitance parameters that are needed for use with Getsinger's data [13] in order to obtain dimensional parameters from electrical parameters are as follows:

$$c_{gi} = C_{gi}/\epsilon$$
$$c_{i,i+1} = C_{i,i+1}/\epsilon$$
$$\epsilon = \epsilon_r\epsilon_0$$

ϵ_r = relative dielectric constant of the medium

ϵ_0 = permittivity of free space in the units of C_{gi} and $C_{i,i+1}$. (2)

The coupling $k_{i,i+1}$, between meander-line turns i and $i+1$ is defined as

$$k_{i,i+1} = -20 \log_{10} \frac{C_{i,i+1}}{\sqrt{(C_{g_1} + C_{i,i+1})(C_{g_{i+1}} + C_{i,i+1})}} \text{ dB}. \quad (3)$$

The meander-line transformer bandwidth BW is defined as

$$\text{BW} = \theta_2/\theta_1 \quad (4)$$

where θ_1 and θ_2 are the lower and upper passband edges, respectively, in electrical degrees or frequency. The ratio of load-to-source resistance, always taken as greater than 1, is denoted by the symbol RL/RG and the peak VSWR in the passband is denoted by VSWR.

A comprehensive table of meander-line transformer designs for $N = 2$ to 6 turns, $RL/RG = 1.0$ to 20.0, and BW = 1.5 to 10 has been deposited with ASIS National Auxiliary Publications Service.[2] For purposes of illustration an extract is presented in Table I.

The normalized self and mutual capacitances are listed under the column headings CGi/E and $CMij/E$, respectively. These values may be converted to the dimensionless forms C/ϵ required by Getsinger's data by the equation

$$\left.\begin{matrix} C_{g_i}/\epsilon \\ \text{or} \\ C_{i,i+1}/\epsilon \end{matrix}\right\} = \frac{376.7}{RG\sqrt{\epsilon_r}} \{\text{Table I value}\} \quad (5)$$

where RG is the source resistance in ohms. Table I was terminated after the peak passband VSWR exceeded 1.5.

B. Discussion of Design Tables

For the data presented in Table I the coupling between meander-line turns was arbitrarily (after some analytical experimentation) required to be within the range 10–16 dB. This range of coupling generally yields a realizable and compact structure for coplanar coupled strips. Tighter than 10-dB coupling tends to become difficult to realize, while less than 16-dB coupling is entering a region that is beginning to sepa-

[2] For detailed tables, order document NAPS 01929, from ASIS National Auxiliary Publications Service, c/o CCM Information Corporation, 866 Third Avenue, New York, N. Y. 10022; remitting $2.00 for each microfiche or $5.00 for each photocopy.

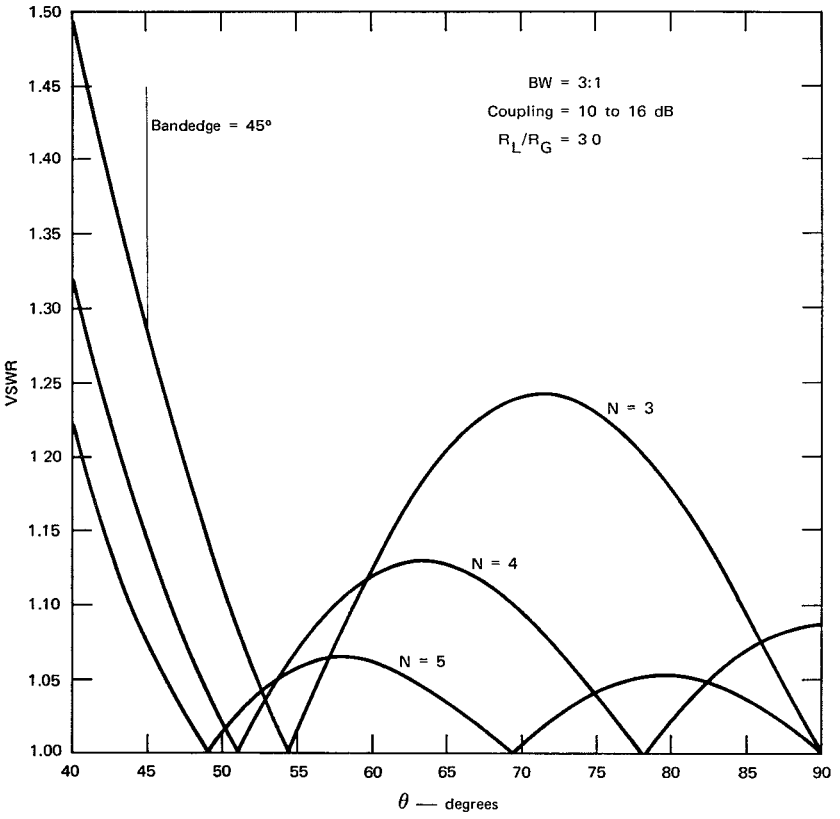

Fig. 7. VSWR versus electrical degrees for N = three-, four-, and five-turn meander-line transformers.

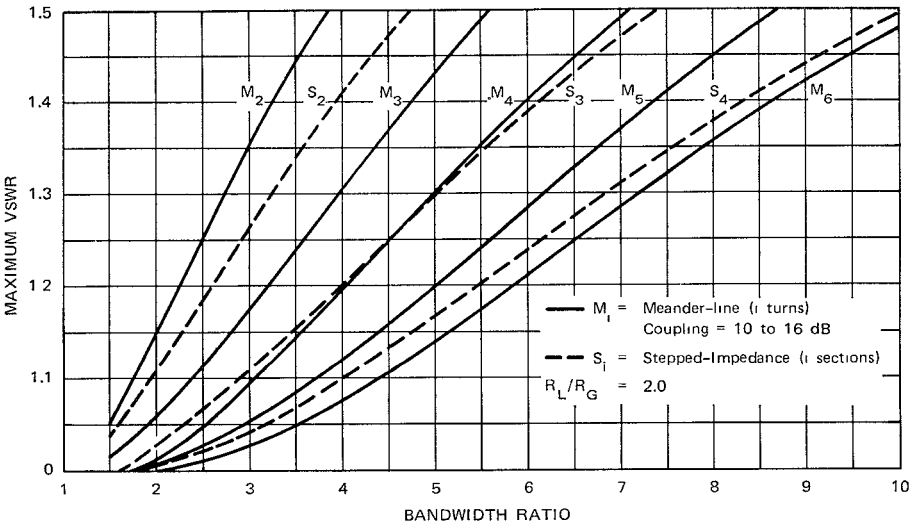

Fig. 8. VSWR versus bandwidth for meander-line and stepped-impedance transformers.

rate the adjacent strips farther than is desirable. Since the effects of the finite-length interconnections between strips were neglected in compiling Table I, the interconnection lengths should be made as small as possible if the measured performance of the transformer is to correspond well with the theoretical performance. In the physical realization of the transformers, compensation of the interconnections will generally be required.

The effects of varying the coupling between meander-line turns are shown in the graph of Fig. 6. This graph is for the particular case of $N=4$ turns, $RL/RG=2$, and BW = 3:1, but is typical of the results in the general case. The graph plots maximum VSWR in the passband as a function of coupling between turns. The horizontal arrow depicts the range of coupling allowed by the computer program. The right-hand sides of the arrows are connected by a smooth curve. This is somewhat arbitrary, but is justified by the fact that coupling values determined by the computer tend toward weaker coupling in most cases. In any event, the qualitative result is the same regardless of the way the curve is connected. The data show that for a given bandwidth the peak VSWR is minimized when the coupling is weakest. Thus, for the class of meander-line transformers, stepped-impedance transformers yield the lowest VSWR's. This is not an especially surprising

TABLE II

EXAMPLE OF FOUR-TURN MEANDER-LINE 3:1 BANDWIDTH TRANSFORMER DESIGN ($RL/RG = 2$)

Conductor	w/b*	s/b†
1 (25 Ω end)	1.550	0.1059
2	1.224	0.1508
3	0.9911	0.1767
4	0.8137	

* w/b = Strip-width-to-ground-plane spacing.
† s/b = Interstrip-spacing-to-ground-plane spacing.

TABLE III

ELECTRICAL AND DIMENSIONAL PARAMETERS FOR AN EXPERIMENTAL STRIPLINE THREE-TURN MEANDER-LINE TRANSFORMER

Line	C_{g_i}/ϵ	$C_{i,i+1}/\epsilon$	Linewidth, w (inch)	Inter-Line Spacing, s (inch)
1 (25-Ω side)	6.7191	1.6005	0.354	0.015
2	4.2162	1.5074	0.246	0.018
3 (50-Ω side)	4.1891		0.196	
Impedance transformation 2:1 Fractional bandwidth 0.60 (BW = 1.857)			Theoretical VSWR = 1.048	

result since the coupling between turns introduces constraints on the physical realizability of the meander line. Also, the same conclusion might be inferred from the data of Wenzel [14], [15], which showed that C-section transformers[3] have smaller bandwidths than stepped-impedance transformers for a given VSWR and number of sections.

Since Table I was developed using numerical techniques, it is worthwhile to examine the responses of the transformers in more detail. Fig. 7 shows typical computed responses for three-, four-, and five-turn meander-line transformers, all having 3:1 bandwidths, 3:1 impedance transformation ratios, and 10–16 dB-coupling between turns. The improvement in VSWR with increasing N is evident. The VSWR's are not quite equal ripple, but on the other hand are so close to equal ripple that the difference is virtually academic. Certainly, in any realization of these designs, the effect of losses, interconnections, and parasitics would completely obscure any differences between these and precisely equal-ripple designs. Note also that the peak VSWR occurs at the bandedge.[4] Since it is the peak VSWR that is given in Table I and since the bandedge performance is almost always degraded in actual hardware realizations, a user may generally assume that the maximum VSWR is slightly lower than that given in Table I over most of the band of application.

Fig. 8 presents representative data of maximum VSWR versus bandwidth BW, with the number of meander-line turns as a parameter. Also plotted are the corresponding data for stepped-impedance transformers. The impedance transformation ratio is 2:1 and the coupling between meander-line turns is 10–16 dB. The data show the superiority of the stepped-impedance transformer with regard to bandwidth. However,

[3] A C-section transformer may also be considered a two-turn meander-line transformer.
[4] This is not always the case, but is usually so.

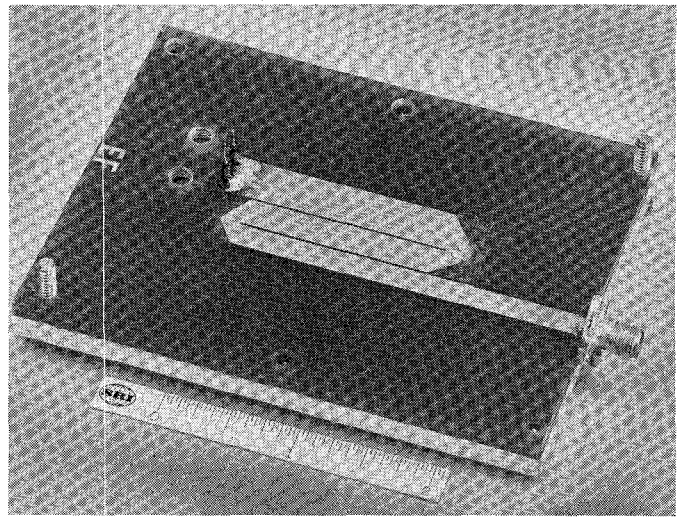

Fig. 9. Photograph of experimental three-turn meander-line transformer.

TABLE IV

ELECTRICAL AND DIMENSIONAL PARAMETERS FOR AN EXPERIMENTAL FOURTH-ORDER STRIPLINE HYBRID MEANDER-LINE TRANSFORMER

Line	C_{g_i}/ϵ	$C_{i,i+1}/\epsilon$	Linewidth, w (inch)	Inter-Line Spacing, s (inch)
1 (25-Ω side)	7.208	1.2300	0.380	0.026
2	6.182	0.0	0.316	
3	5.2792	0.9006	0.253	0.043
4 (50-Ω side)	4.5239		0.206	

equivalent or greater bandwidth is always possible with meander-line transformers by adding additional turns. Again, we reiterate that the principal advantage of meander-line and hybrid meander-line transformers is the reduction in overall length and the increased flexibility in obtaining suitable shape factors for the stripline or MIC transformers being considered.

C. Example Design

The use of the meander-line transformer design tables (Table I) will be illustrated in the following example. It is required to match 25–50 Ω over a 3:1 bandwidth. The maximum VSWR allowed is 1.1. Checking Table I for $RL/RG = 50/25 = 2$ and for $N = 3$ and 4 shows that the maximum VSWR's are 1.288 and 1.095, respectively. Thus $N = 4$ turns is sufficient. The parameters from the $N = 4$, BW = 3:1 tables are as follows:

$$\begin{aligned} CG1/E &= 0.7757 \\ CG2/E &= 0.5699 \\ CG3/E &= 0.4826 \\ CG4/E &= 0.4744 \\ CM12/E &= 0.1298 \\ CM23/E &= 0.1041 \\ CM34/E &= 0.09295. \end{aligned} \tag{6}$$

We will assume that the transformer is to be constructed in stripline on 1-oz copper-clad Rexolite 1422, which has a relative dielectric constant of 2.54. Since the tables are calculated

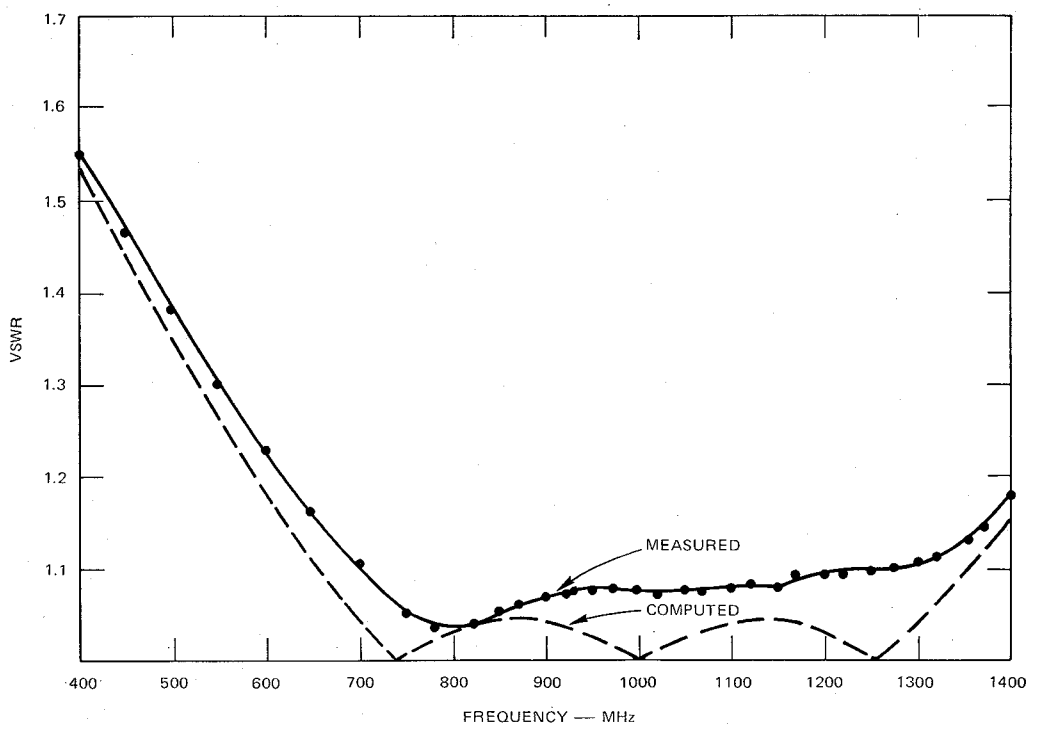

Fig. 10. Measured and computed VSWR's for experimental three-turn meander-line transformer.

Fig. 11. Measured reflection coefficient on a Smith chart overlay for the experimental three-turn meander-line transformer.

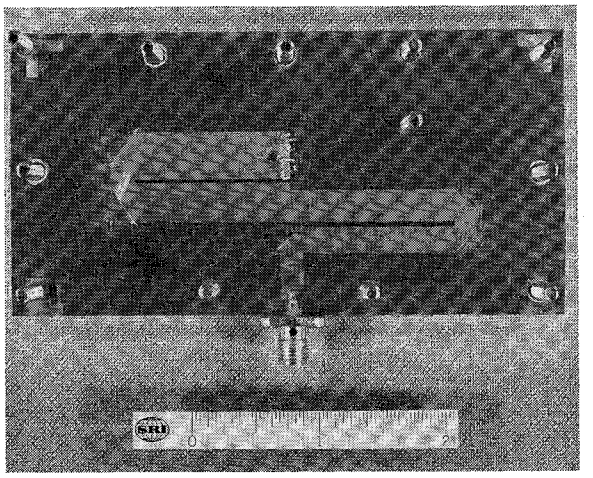

Fig. 12. Photograph of an experimental $N=4$ hybrid meander-line transformer.

on the basis that the "load" is always greater than the source, the generator resistance in this case is identified as 25 Ω. Consequently, substituting (6) into (5) yields

$$C_{01}/\epsilon = \frac{376.7}{25\sqrt{2.54}}\{0.7757\} = 9.454(0.7757) = 7.334$$

$$C_{02}/\epsilon = 9.454(0.5699) = 5.388$$

$$C_{03}/\epsilon = 9.454(0.4826) = 4.563$$

$$C_{04}/\epsilon = 9.454(0.4744) = 4.485$$

$$C_{12}/\epsilon = 9.454(0.1298) = 1.227$$

$$C_{23}/\epsilon = 9.454(0.1041) = 0.9842$$

$$C_{34}/\epsilon = 9.454(0.09295) = 0.8788. \quad (7)$$

Substituting (7) into Getsinger's data yields the results given in Table II.

III. Experimental Results

A. Three-Turn Meander-Line Transformer

A three-turn meander-line transformer was designed to match a 25-Ω load to a 50-Ω source over a 60-percent bandwidth (BW = 1.857). It was constructed in stripline using 1-oz copper-clad Rexolite 1422, and a ground-plane spacing of 0.250 in. The electrical and dimensional parameters are given in Table III. The nominal center frequency was 1 GHz. The interconnections between meander-line turns were mitered experimentally for a satisfactory VSWR. Four 1/8-W 100-Ω carbon resistors connected in parallel were used for the 25-Ω load. A photograph of the final design is given in Fig. 9. The measured and computed VSWR's are shown in Fig. 10. Note that although the center frequency of the transformer is

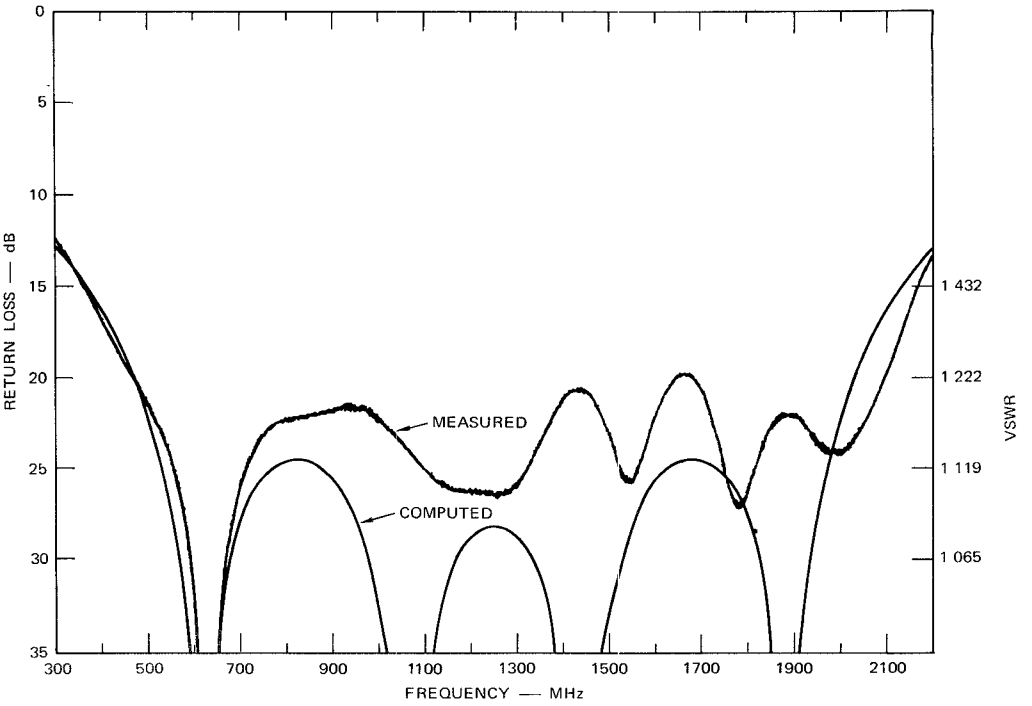

Fig. 13. Measured and computed return loss for experimental $N=4$ hybrid meander-line transformer.

slightly high and although there is some degradation in the response near the upper bandedge, generally speaking, there is excellent agreement between the two curves. Also, a photograph of the measured reflection coefficient from 400 to 1400 MHz is shown on an expanded Smith chart overlay in Fig. 11.

B. Fourth-Order Hybrid Meander-Line Transformer

In order to confirm the theory and design procedure for hybrid meander-line transformers, an $N=4$ hybrid transformer covering a 4:1 bandwidth and matching 25–50 Ω was designed. The theoretical peak VSWR for the hybrid is 1.14. This transformer was also constructed in stripline using 1-oz copper-clad Rexolite 1422 and a ground-plane spacing of 0.250 in. Its nominal center frequency was 1.250 GHz. The electrical and dimensional parameters are given in Table IV and a photograph of the transformer after the interconnections were mitered is given in Fig. 12. The measured and computed return loss is given in Fig. 13. Although the measured data at the high-frequency end of the passband indicate that the interconnections are not completely compensated, nevertheless, the mean return loss is about 23 dB. Hence the correspondence with the theory is very good.

IV. Conclusions

A comprehensive table of meander-line transformer designs having from 2 to 6 turns, impedance transformation ratios of from 1.1 to 20, and bandwidth ratios of from 1.5:1 to 10:1 has been deposited with the ASIS National Auxiliary Publications Service. The transformer responses are, for all practical purposes, equal-rippled responses. For a given ripple, the bandwidth of meander-line transformers is less than that of stepped-impedance transformers of the same degree. However, the principal advantage of meander-line transformers is their compactness.

The concept of hybrid meander-line transformers was introduced. Hybrid meander-line transformers permit circuit designers considerable flexibility in choosing the geometrical shape of the transformer design. The bandwidth of hybrid transformers lies between that of meander-line and stepped-impedance designs for the same passband VSWR. Several examples of hybrid transformers were illustrated in the text.

Experimental three-turn meander-line and $N=4$ hybrid meander-line transformers were designed and constructed in stripline. The experimental data compared favorably with the theoretically computed responses.

Acknowledgment

The author wishes to thank Dr. U. Gysel for several illuminating discussions concerning the numerical methods used to obtain the meander-line design table and for allowing the author the use of his modified computer program of the Fletcher–Powell technique for minimization of a function of several variables. The author would also like to acknowledge the excellent work done by E. Fernandes, who accurately constructed and measured the experimental meander-line transformers.

References

[1] G. L. Matthaei, L. Young, and E. M. T. Jones, *Design of Microwave Filters, Impedance-Matching Networks, and Coupling Structures.* New York: McGraw-Hill, 1964.
[2] R. E. Collin, "Theory and design of wide-band multisection quarter-wave transformers," *Proc. IRE*, vol. 43, pp. 179–185, Feb. 1955.
[3] H. J. Riblet, "General synthesis of quarter-wave impedance transformers," *IRE Trans. Microwave Theory Tech.*, vol. MTT-5, pp. 36–43, Jan. 1957.
[4] L. Young, "Tables for cascaded homogeneous quarter-wave transformers," *IRE Trans. Microwave Theory Tech.*, vol. MTT-7, pp. 233–237, Apr. 1959.
[5] H. Ozaki and J. Ishii, "Synthesis of transmission-line networks and the design of UHF filters," *IEEE Trans. Circuit Theory*, vol. CT-2, pp. 325–335, Dec. 1955.
[6] G. L. Matthaei, "Short-step Chebyshev impedance transformers," *IEEE Trans. Microwave Theory Tech.*, vol. MTT-14, pp. 372–384, Aug. 1966.
[7] P. N. Butcher, "The coupling impedance of tape structures," *Proc. Elec. Eng.*, vol. 104, pt. 8, pp. 177–187, Mar. 1957.
[8] J. T. Bolljahn and G. L. Matthaei, "A study of the phase and filter properties of arrays of parallel conductors between ground planes," *Proc. IRE*, vol. 50, pp. 299–311, Mar. 1962.

[9] H. S. Hewitt, "A computer designed 720 to 1 microwave compression filter," *IEEE Trans. Microwave Theory Tech.*, vol. MTT-15, pp. 687–694, Dec. 1967.
[10] R. Sato "A design method for meander-line networks using equivalent circuit transformations," *IEEE Trans. Microwave Theory Tech.*, vol. MTT-19, pp. 431–442, May 1971.
[11] P. I. Richards, "Resistor transmission-line circuits," *Proc. IRE*, vol. 36, pp. 217–220, Feb. 1948.
[12] J. W. Bandler, "Optimization methods for computer-aided design," *IEEE Trans. Microwave Theory Tech.*, vol. MTT-17, pp. 533–552, Aug. 1969.
[13] W. J. Getsinger, "Coupled rectangular bars between parallel plates," *IRE Trans. Microwave Theory Tech.*, vol. MTT-10, pp. 65–73, Jan. 1962.
[14] R. J. Wenzel, "Small elliptic-function low-pass filters and other applications of microwave *C* sections," *IEEE Trans. Microwave Theory Tech.*, vol. MTT-18, pp. 1150–1158, Dec. 1970.
[15] G. I. Zysman and A. Matsumoto, "Properties of microwave *C*-sections," *IEEE Trans. Circuit Theory*, vol. CT-12, pp. 74–82, Mar. 1965.

Efficient Capacitance Calculations for Three-Dimensional Multiconductor Systems

ALBERT E. RUEHLI AND PIERCE A. BRENNAN

Abstract—**The design and packaging of integrated circuits requires the calculation of capacitances for three-dimensional conductors located on parallel planes. An integral-equation (IE) computer-solution technique is presented, which provides accurate results. The solution technique minimizes computer storage requirements while maintaining calculating efficiency without excessive computation times.**

I. Introduction

IN THE PAST, integral-equation (IE) techniques found extensive use in capacitance calculations for two-dimensional geometries [1]–[7]. These solutions have proven to be very useful for systems involving sets of long parallel transmission lines (conductors) in a multidielectric environment. Further, for sufficiently high frequencies and TEM-mode propagation, the characteristic impedance can be found [8]. Thus all electrical parameters required for a complete characterization of a set of low-loss transmission lines are obtainable from the IE approach.

Three-dimensional capacitance calculations, however, have been limited to small problems. The capacitance of an infinitely thin square plate has been considered by several authors [9]–[13], while the capacitance between parallel plates [14] and for a cube has been found [15]. Recently, solutions have been obtained for problems involving infinite dielectric regions [16]–[18] by using Green's function techniques similar to those used in the two-dimensional calculations cited above.

The numerical solution of the IE leads to a matrix that resembles the coefficients of potential for multiconductors. In a two-dimensional analysis, the unknowns represent the surface charge (on the boundary of a cross section), and are therefore one dimensional. Approximately 30 unknowns lead to a good solution for an average problem on a small computer since the matrix requires only 900 words of storage.

Manuscript received May 30, 1972; revised July 28, 1972.
The authors are with the IBM Thomas J. Watson Research Center, Yorktown Heights, N. Y. 10598.

In contrast to this, the unknowns representing the surface charge will be two dimensional when the IE approach is applied to a three-dimensional capacitance problem. If the above example is extended to this case, matrices larger than 1000×1000 result, requiring excessive storage for a direct matrix inversion. This presents a serious limitation to three-dimensional calculations especially since the matrices are full. The solutions introduced here considerably reduce storage requirements for the matrix of coefficients without unduly increasing computation complexity, allowing the treatment of three-dimensional conductors on multiple planes.

In some situations, the presence of closely spaced ground planes makes a two-dimensional description [1]–[7] possible, and thus a transmission-line characterization suffices. However, if ground planes are remote or not present, three-dimensional solutions become necessary. Specifically, the use of partial capacitances (defined later) in conjunction with partial inductances [19] leads to a three-dimensional technique, and partial-element equivalent circuits [20] result in a complete characterization of three-dimensional interconnection structures.

In Section II, the formulation of the IE solution is developed, while Section III is devoted to the numerical solution. In Section IV, the evaluation of the coefficient matrix is considered, and in Section V, Green's functions for the inclusion of infinite interfaces are considered. Important relations to multicapacitance concepts are established in Section VI, while comparisons with other results are made in Section VII.

II. Integral-Equation Formulation

A set of K conductors is considered with or without infinite ground planes or with infinite dielectric regions present. The potential $\Phi(\bar{r}_i)$ at a field point $\bar{r}_i$ in the system is

$$\Phi(\bar{r}_i) = \sum_{k=1}^{K} \int_{s_k} G(\bar{r}_i, \bar{r}') q(\bar{r}')\, ds' \qquad (1)$$

where q is the charge density on the conductor surfaces s_k and